# Nonlinear fractional dynamics integrated physics-informed neural network model for LiFePO<sub>4</sub> batteries in electric vehicles

Manashita Borah, Shida Jiang, Junzhe Shi, Scott Moura

Abstract— This paper addresses the long-standing challenge of attaining high-precision models for LiFePO<sub>4</sub> batteries which suffer from weakly observable dynamics. We introduce a new paradigm of integrating a nonlinear fractional-order physicsbased model with a hybrid neural network model. First, a fractional-order model (FOM) is proposed to capture the physics of the battery that existing integer-order models (IOMs) fail to replicate, such as the solid phase diffusion. The FOM parameters are state dependent as they vary along with the progression of the state of charge (SOC). Second, the unknown and unmodelled physics is captured by a hybrid neural network model integrated with the FOM. The physical states of the FOM are used to guide the neural network resulting in a state dependent nonlinear fractional-order physics-informed neural network (FO-PINN) to predict the terminal voltage of the battery. Validation with experimental results and comparisons with existing modelling techniques reveal that the proposed scheme delivers improved predictive accuracy with decreased computational cost and enhanced physically meaningful information. The scheme has potential in applications that demand high propulsive power and accuracy, such as electric aircraft.

# I. INTRODUCTION

Lithium-ion batteries (LIBs) play a pivotal role in catalysing a zero-carbon future. Electric vehicles, propelled by LIBs, are revolutionising the automotive industry by significantly reducing greenhouse gas emissions and urban air pollution. These batteries may enable effective integration of renewable sources like solar and wind into our energy mix, providing a dependable energy supply when the sun does not shine, and the wind does not blow. However, there are still bottlenecks in these pursuits of a carbon- neutral, sustainable future facilitated by LIBs. A crucial challenge is accurate modelling of batteries. To harness the full potential of LIBs, it is essential to develop precise and comprehensive models that can predict their behaviour under various operating conditions; still a major limitation in battery technology.

#### A. Literature survey

The existing LIBs used in high-end Electric vehicles (EVs), such as the Nickel-Manganese-Cobalt batteries, suffer from technical bottlenecks of safety, reliability, cost, lifespan, lack of real-time measurements, parametric uncertainties, and limited supply of raw material. The industry is now actively looking for alternative LIBs that are cheaper, more reliable, can be sourced locally and have longer lifespan such as the Lithium Ferrous Phosphate (LFP) batteries. Recently, the

automotive industry is moving towards utilising LFP for powering their EVs. [1]. Battery manufacturers are investing significantly to the production of LFP batteries [2]. Global production of LFP batteries is forecast to be 770 GWh by 2025, that is about one-third of all battery capacity [3]. These point towards LFP emerging as the future energy storage system. However, this transition to LFP battery is encountering hurdles, primarily due to some of its inherent limitations. One of them is the scarcity of high accuracy and economically viable battery models, crucial for their optimised performance, safety and diagnosis.

Current battery models can be broadly categorised into physics-based models (PBMs) and machine learning models (MLMs). PBMs of batteries may be further classified into electrochemical models and equivalent circuit models [4]. Some of the challenges for battery modelling are pointed out below:

- Extensive computational efforts, and complexity of electrochemical models like Doyle- Fuller-Newman or single particle models, where they require tens of parameters to be designed.
- ii. MLMs are black box models that generally do not reflect physically meaningful information, thus limiting their use for physical state estimation. Besides, they require large datasets for training.
- iii. Though equivalent circuit models have low computational burden, they fail to represent important battery phenomena such as charge transfer reaction, solid phase diffusion and the double layer effect.
- iv. Additionally, most of these existing models are defined by constant parameters that are often unable to capture nonlinear phenomena in battery dynamics. This contributes to the weakly observable dynamics of the LFP battery, making it difficult to estimate SOC.

The above drawbacks clearly signify that neither PBM nor MLM alone can solve the challenges of battery prediction and estimation. In *Nature Reviews* article, a new concept of physics-informed machine learning (PIML) was reported [5], so that the tedious training networks involving big data can be reduced using the information provided by the laws of physics, even in partially understood, uncertain systems, and scalable to large problems. Due to its said advantages, PIML has drawn attention in the battery research community to study dynamics

M. Borah in this work is supported by Fulbright fellowship and industry-academia project grant from TotalEnergies (Agreement Number 20163367) at University of California, Berkeley, USA.

M. Borah\*, J. Shi, S. Jiang, S. Moura are with the Department of Civil and Environmental Engineering, University of California, Berkeley, USA (phone:

5102921812; e-mail: \*manashitaborah@berkely.edu; manashitaborah@gmail.com).

M. Borah is also with Department of Electrical Engineering, Tezpur University, Assam, India, 784028

such as degradation, state of health [6], thermal runaway and conductivity [7,8], thrust compensation [9], random-load discharge and aging prediction [10]. In terms of PIML application to voltage prediction models of batteries, Li et al. [11] used PIML to model potentials of electrolyte concentration, electrode and electrolyte for NMC battery chemistry. In 2023, Tu et al. [4] designed a PIML composed of a nonlinear double capacitor PBM to inspire a feedforward neural network to predict terminal voltage in LIBs. However, these voltage prediction models are confined to integer-order models and chemistries other than LFP.

Integer-order equivalent circuit PBMs, defined by ideal capacitors and inductors may not accurately capture the system behaviour when the relationship between voltage and current is not precisely an integral derivative [12]. These "non-ideal" relationships, such as solid phase diffusion and double layer effect can be captured by a fractional-order (FO) capacitor or an FO inductor [13, 14]. Very recently in 2022, fractional calculus integrated with PIML for estimating states in LIBs is reported and found to deliver improved convergence speed [15, 16]. The FOMs used in these works are defined by fractional-order partial differential equations and the methodologies are tested on NMC battery. So far, a PIML framework integrated with a FOM defined by state dependent fractional order differential equations to predict terminal voltage of a battery is not found in literature. This paper addresses that gap.

# B. Contribution of this paper

The novel contributions of the paper are:

i. Though FOMs of batteries have been reported in literature, an SOC dependent nonlinear FOM has not been reported so far to the best of the authors' knowledge.

The FOM proposed has been experimentally validated to effectively capture fractional dynamics, such as solidphase diffusion which conventional IOMs struggle to encompass. Additionally, the FOM utilises state dependent parameters to capture nonlinearities more accurately.

ii. A physics-informed neural network (PINN) architecture for modelling batteries that combines a fractional-order differential equation model with a hybrid neural network is new.

The integration of the hybrid neural network with the FOM accounts for the unknown and unmodelled aspects of the underlying battery physics.

iii. The modelling framework is applied to an LFP battery, which is challenged by weakly observable dynamics, and existing PINN strategies in literature are mostly confined to NMC and LCO battery chemistries.

# C. Organisation

The remainder of the paper is organised as follows. Section II introduces the state dependent nonlinear FOM, and its parameter identification along with some preliminaries of FO calculus. Section III describes the nonlinear FO-PINN architecture. Section IV reports the results, and the paper is concluded in Section V.

# II. STATE DEPENDENT NONLINEAR FRACTIONAL-ORDER MODEL

This section commences with the fundamentals of fractional calculus, followed by development of the proposed state dependent nonlinear FOM.

### A. Fundamentals of fractional-order calculus

The Caputo fractional derivative of order  $\alpha$  of a continuous function f(t) is defined as in (1) [17].

Tunction 
$$f(t)$$
 is defined as in (1) [17]. 
$$D_t^{\alpha} f(t) = \frac{d^{\alpha} f(t)}{dt^{\alpha}} = \begin{cases} \frac{1}{\Gamma(m-\alpha)} \int_0^t \frac{f^{(m)}(\tau)}{(t-\tau)^{\alpha-m+1}} d\tau, & m-1 < \alpha < m, m \in \mathbb{N} \\ \frac{d^m}{dt^m} f(t), & \alpha = m \end{cases}$$
 The Laplace transform of the Caputo fractional derivative in

$$L\left\{\frac{d^{\alpha}f(t)}{dt^{\alpha}}\right\} = s^{\alpha}L\{f(t)\} - \sum_{k=0}^{m-1} s^{\alpha-k-1}f^{(k)}(0)$$
 (2)

A generalized fractional-order nonlinear system is defined as in (3),

$$D_t^{\alpha} x_i(t) = f_i(x(t), t), \tag{3}$$

where the FOs lie in 
$$0 < \alpha < 1$$
 and  $x(t) = [x_1, x_2, ..., x_n]^T$ ,  $(i = 1, 2, ..., n)$ .

The computation of the above fractional-order differential equation is carried out using Adams-Bashforth-Moulton method based on the predictor-corrector technique [18]. The system (3) may be written as a Volterra integral equation as,

$$x_i(t) = x_i(0) + \frac{1}{\Gamma \alpha} \int_0^t (t - \tau)^{\alpha - 1} f_i(x_1, x_2, \dots, x_n) d\tau,$$
 where  $x_i(0)$  are the initial conditions of  $x_i(t)$ .

The corrector equation obtained by substituting  $h = \frac{T}{N}$ ,  $t_n =$ nh, for (n = 0,1,...,N) for a unique solution in [0,T] is (5),

$$x_{ih}(t_{n+1}) = x_i(0) + \frac{h^{\alpha}}{\Gamma(\alpha+2)} f_i\left(x_{1h}^p(t_{n+1}), x_{2h}^p(t_{n+1}), \dots, x_{nh}^p(t_{n+1})\right) + \frac{h^{\alpha}}{\Gamma(\alpha+2)} \sum_{i=1}^{n} a_{i,j,n+1} f_i\left(x_1(t_j), x_2(t_j), \dots, x_n(t_j)\right)$$
where

where, 
$$\begin{aligned} a_{i,j,n+1} &= \\ & \begin{cases} n^{\alpha+1} - (n-\alpha)(n+1)^{\alpha}, & \text{if } j=0 \\ (n-j+2)^{\alpha+1} + (n-j)^{\alpha+1} - 2(n-j+1)^{\alpha+1}, & \text{if } 1 \leq j \leq n \\ 1, & \text{if } j=n+1 \end{aligned}$$

The predicted value  $x_{ih}^p(t_{n+1})$  is determined by

$$x_{ih}^{p}(t_{n+1}) = x_{i}(0) + \frac{1}{\Gamma(\alpha)} \sum_{j=0}^{n} b_{i,j,n+1} f_{i}\left(x_{ih}(t_{j})\right), \tag{6}$$

where  $b_{i,j,n+1} = \frac{h^{\alpha}}{\alpha}((n-j+1)^{\alpha} - (n-j)^{\alpha}), 0 \le j \le n.$ 

The error estimation is

$$e = \max\{\max\{x_1(t_j) - x_{1h}(t_j)|, \max|x_2(t_j) - x_{2h}(t_j)|, \dots, \max|x_n(t_j) - x_{nh}(t_j)|\} = O(h^{\rho}),$$
where  $j = (0,1,2,\dots,N), \rho = \min\{2,1+\alpha\}.$  (7)

Based on the above preliminaries, we propose the FOM of an LIB in the following subsection.

### B. Proposed FOM as the PBM

A nonlinear fractional-order model of an LIB is defined as  $D^{\alpha}x(t) = g(x,u)$ (8)

$$y = h(x, u) \tag{9}$$

where x is the vector containing the unmeasurable states,  $x = [x_1, x_2, ..., x_n]^T$ , (i = 1, 2, ..., n), u and y are measurable input and output vectors and the fractional orders  $\alpha \in (0,1] = [\alpha_1, \alpha_2, ..., \alpha_n]^T$ .

# C. System identification

The FOM of a battery is constructed conceptually based on electrochemical impedance spectroscopy (EIS). EIS involves measuring the impedance of a battery by applying a small alternating current and observing the response in terminal voltage. The impedance spectrum, represented as a Nyquist plot, is then divided into three distinct frequency regions: low (associated with solid-phase diffusion), mid (related to charge transfer reactions and double layer effects), and high (indicative of ohmic polarization). In the low-frequency region of the Nyquist plot obtained from the EIS experiment, a fractional-order circuit element known as the constant phase element (CPE) is employed for modelling. The key unique feature of CPE is its ability to take on non-integer values, which makes it suitable for capturing the dynamics associated with solid-phase diffusion more accurately compared to an ideal integral capacitor. The resulting fractional-order equivalent circuit model is illustrated in Fig. 1.

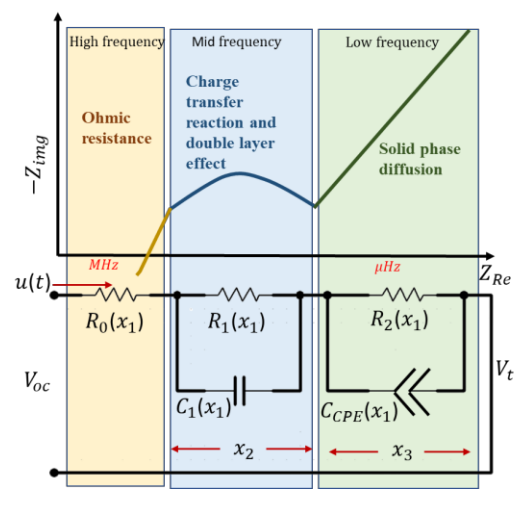


Figure 1. Proposed FOM to capture the dynamics of the EIS spectrum.

The corresponding equations of the proposed FOM in Fig.1 and from (8) and (9) are represented in (10) and (11),

$$\begin{cases} D^{\alpha_1} x_1(t) = -\frac{u(t)}{Q} \\ D^{\alpha_2} x_2(t) = -\frac{1}{R_1(x_1)C_1(x_1)} x_2(t) + \frac{1}{C_1(x_1)} u(t) \\ D^{\alpha_3} x_3(t) = -\frac{1}{R_2(x_1)CPE(x_1)} x_3(t) + \frac{1}{R_2(x_1)CPE(x_1)} u(t) \end{cases}$$

$$y = V_t$$

$$\text{where } V_t = V_{oc}(x_1) - x_2(t) - x_3(t) - R_0(x_1)u(t).$$

$$(11)$$

The fractional orders are  $\alpha = \{\alpha_1, \alpha_2, \alpha_3\} = \{1, 1, \alpha_3\}$ . The state vector  $x = [x_1 \ x_2 \ x_3]^T$  is such that  $x_1 = SOC$ ,  $x_2$  is the voltage across the  $R_1C_1$  pair and  $x_3$  is the voltage across the  $R_2CPE$  pair. The terms  $V_{oc}$  and  $V_t$  are open circuit and terminal voltages of the battery, respectively. Parameter Q is the battery nominal capacity, u is the input current which is

positive for discharging and negative for charging operations.

After conducting the frequency domain experiment, the parameter identification process for the aforementioned FOM described in equations (10) and (11) is carried out using global optimisation technique. In the case of the LFP battery, it is subjected to a Hybrid Pulse Power Characterization (HPPC) or any pulse load current for each 10% drop in SOC, followed by a 10-minute resting period. This cycle is repeated until the battery reaches its lower cut-off voltage. During the resting period, the terminal voltage  $V_t$  is recorded, providing the open-circuit voltage  $V_{oc}$ . From the  $V_{oc}$  measurements, a corresponding relationship of measurements at various SOC levels, i.e.,  $V_{oc}(x_1)$  is derived. Subsequently, an optimisation problem is formulated to minimise the error between the experimental output terminal voltage and the model output voltage, as defined in equation (12).

$$\min e(\hat{\theta}) = \frac{1}{q} \left[ \sum_{k=1}^{q} (V_{t(exp)}(t_k) - V_{t(FOM)}(t_k))^2 \right]^{\frac{1}{2}}$$
(12)

In (12),  $V_{t(exp)}(t_k)$  and  $V_{t(FOM)}(t_k)$  are the experimental terminal voltage and the FOM terminal voltage obtained at  $k^{th}$  sample and  $\theta = [R_0, R_1, R_2, C_1, CPE, \alpha_3]$  represents the set of parameters to be optimised. The identified parameters are nonlinear functions dependent on SOC. The implementation details are provided in Section IV-A.

# III. NONLINEAR FRACTIONAL-ORDER PHYSICS-INFORMED NEURAL NETWORK

In the last section, we introduced the state dependent nonlinear FOM as the PBM that will generate the required physical states to guide the neural network algorithm. In the present section we focus on the structure and architecture of the FO-PINN.

# A. Structure of the Neural Network

Unlike traditional feedforward neural networks used to model batteries in literature [4], recurrent neural networks (RNNs) use hidden nodes to store information of past inputs, thereby encoding time dynamics. However, conventional RNNs use gradient based training and fail to tackle long term dependency. Long-short term memory networks (LSTMs) are a variant of RNN that uses hidden memory instead of hidden nodes to overcome the above hurdle [19]. They have a memory cell that can store and retrieve information over long sequences. This memory capability makes them suitable to capture the unknown physics of the battery varying dynamically with time. A structural cell of LSTM is illustrated in Fig. 2 and described in (13).

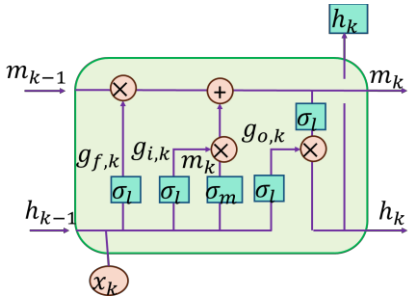


Figure 2. Schematic cell structure of LSTM

$$\begin{cases} g_{f,k} = \sigma_l(w_f x_k + v_f h_{k-1} + b_f) \\ g_{i,k} = \sigma_l(w_i x_k + v_i h_{k-1} + b_i) \\ g_{o,k} = \sigma_l(w_o x_k + v_o h_{k-1} + b_o) \\ m_k = g_{f,k} \odot m_{k-1} + g_{i,k} \odot \sigma_m(w_m x_k + v_m h_{k-1} + b_m) \\ h_k = o_k \odot \sigma_h(c_k) \end{cases}$$
(13)

In (13),  $g_{f,k}$ ,  $g_{i,k}$ ,  $g_{o,k}$  represent the forget, input and output gates, respectively;  $m_k$  is the hidden unit memory;  $x_k$  is the unit input;  $h_k$  is the unit output, all at instant k;  $\sigma_l$  is the logistic sigmoid function,  $\sigma_m$  and  $\sigma_h$  are hyperbolic tangent functions;  $\odot$  is the Hadamard product; w, v, b are weight matrices and bias parameters updated during training.

LSTMs are designed to handle long-range dependencies in sequences, making them well-suited for tasks involving time series data. Convolutional neural networks (CNNs), on the other hand, are designed to capture spatial hierarchies and local patterns in data. They use convolutional layers to scan small local regions of the input data and learn features that are shared across the entire pattern. The activation function for a 1-dimensional CNN layer is described in (14),

$$h_k = \sigma_{cnn}(w_{cnn} * x_k + b_{cnn}) \tag{14}$$

where, \* is the convolution operation between the input signal  $x_k$  and the filter weight  $w_{cnn}$ ;  $b_{cnn}$  is a bias parameter;  $\sigma_{cnn}$  is the underlying activation function.

We adopt a hybrid neural network model that can leverage the strengths of both CNNs and LSTMs. To elaborate, by employing a CNN as the initial layer of the model, the sophisticated spatial characteristics from the initial data can be extracted. The output of the CNN layers is then fed as input to LSTM layers, to provide the LSTM with a more semantically rich representation of the data, helping the LSTM focus on temporal dependencies within these features. The LSTM component is employed to characterise the connections between the current battery dynamics and past input data. This innovative network architecture capitalises on the strengths of both the CNN and LSTM networks, enabling the simultaneous capture of spatial and temporal features within battery data. The CNN-LSTM structure of hybrid neural network is designed to model the unknown battery physics by processing the hierarchical spatial features extracted from the CNN while also considering the temporal context from the LSTM. Furthermore, CNN-LSTM is reported to have improved prediction capabilities for LIB state estimation when compared with either CNN or LSTM [20].

# B. Architecture of the FO-PINN model

Two broad classifications of PIML architectures are outlined in [21]: i) sequentially integrated models and ii) hybridised PBM and MLMs. We present the architecture of residual or delta learning which is a type of sequential integration PIML model. Here, PBM is an integral part of the prediction pipeline, while the MLM learns the difference or the residue between the PBM and the experimental output.

As shown in the architecture of Fig.3, the PBM is the state dependent nonlinear FOM of the LIB detailed in Section II-A. The MLM is a hybrid neural network of CNN-LSTM neural network described in Section III-A. The output of the FOM is  $V_{t(FOM)}$ . The CNN-LSTM learns the residual of the FOM

 $\Delta V = V_{t(exp)} - V_{t(FOM)}$  to deliver the final predicted voltage as,  $V_{t(FO-PINN)} = V_{t(FOM)} + \Delta V$  (15).

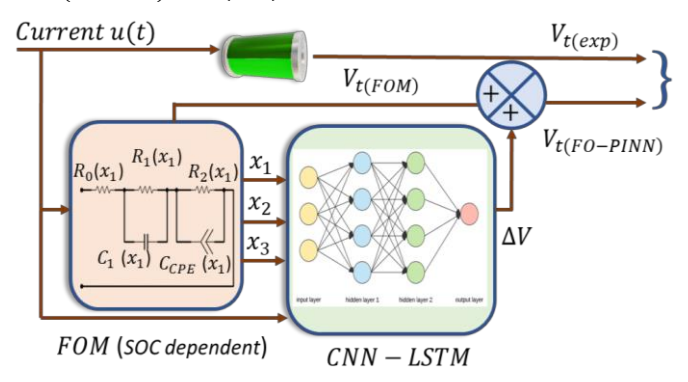


Figure 3. Architecture of FO-PINN based on sequential residual learning.

The implementation of the architecture above to predict LIB terminal voltage is presented in Section IV.

# IV. RESULTS AND DISCUSSIONS

The results are elucidated in the following subsections, beginning with the parameter identification of the SOC dependent nonlinear FOM followed by its integration with the neural network to predict the terminal voltage of the LFP battery.

# A. Model validation with identified parameters

The laboratory setup for experimentation is shown in Fig.

4

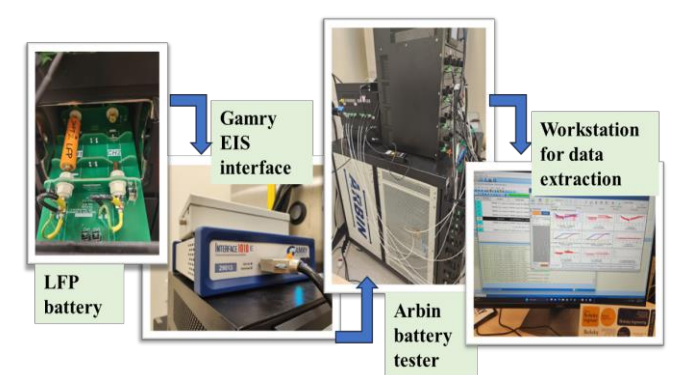


Figure 4. Experimental set up.

EIS experiments are conducted in a Gamry1010E instrument. It is interfaced with a workstation that processes the data. Fresh 18650 LFP cells of 3.3 V nominal voltage, 1.2 Ah capacity are taken for testing. The input to the EIS is an alternating current of 0.1 A and the frequency spectrum is varied from 0.01 Hz to 100 kHz at 25° C. The Nyquist plot derived from the EIS is plotted in green and the fitted models in purple in Fig. 5. This validates our first claim of contribution that the FOM with SOC dependent parameters captures the solid phase diffusion dynamics at low frequency better than that by an IOM with constant parameters. Although it also outperforms IOM with SOC dependent parameters, we have omitted the detailed presentation due to limitations in the available space.

The parameter identification detailed in Section II-C is carried out using chaos-based Particle Swarm optimisation, where the

cost function is optimised with respect to three indices: position, speed and fitness.

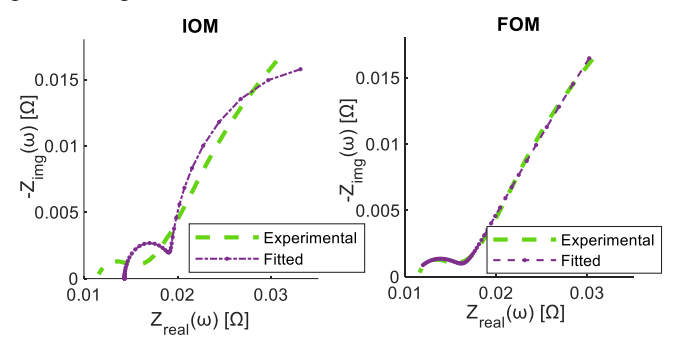


Figure 5. Comparison of the proposed FOM with the IOM against experimental data in frequency spectrum from the EIS experiment

The hyperparameters are chosen as the dimension of six representing the six parameters to be optimized:  $R_0$ ,  $R_1$ ,  $R_2$ ,  $C_1$ , CPE and  $\alpha_3$ , acceleration factor =0.1, minimum inertia weight 0.5, maximum inertia weight =1, population size =50 and number of generations=500. The parameters are optimised using (12) for each 10% decay between 0 and 100% SOC inclusive.

# B. Voltage prediction of LFP battery using proposed scheme

The input to the SOC dependent nonlinear FOM is an Urban Dynamometer Driving Schedule (UDDS) current profile u(t), shown in Fig 6 a). The fractional-order differential equations of (10) are solved using Caputo derivative (1) with the help of the numerical method described in (4)-(7). The solutions of the equations are the physical states:  $x_1, x_2$  and  $x_3$  which are then used to compute the simulated model voltage  $V_{t(FOM)}$  using (11). The physical states  $x_1, x_2$  and  $x_3$  are plotted in Figs. 6 b)- 6 d). They are fed as input to the first layer of the hybrid neural network, i.e. CNN using the architecture described in Section III-B and III-C.

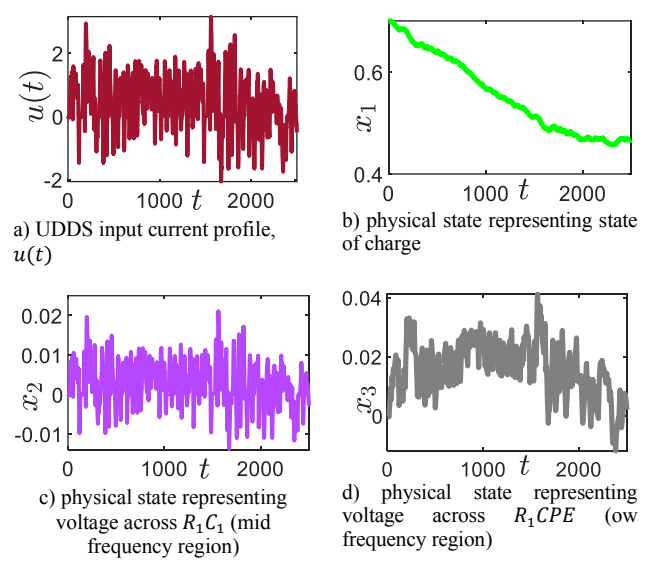
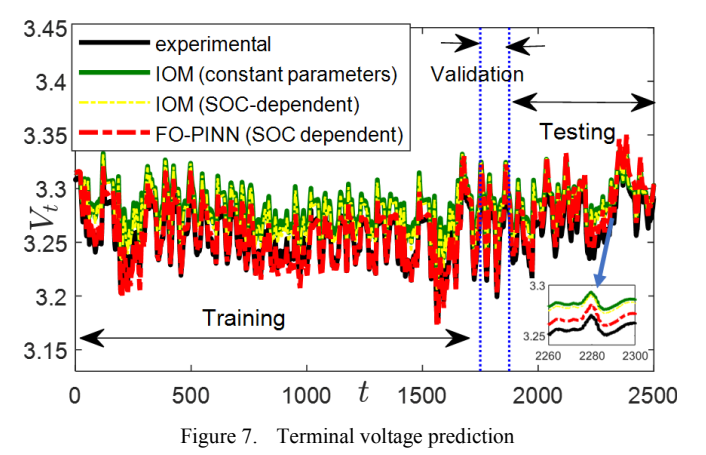


Figure 6. Inputs (current and physical states) to the FO-PINN.

The CNN layer is designed with six filters of length three that extract the spatial hierarchies and local pattern of the input data i.e. u(t),  $x_1$ ,  $x_2$  and  $x_3$ . While increasing the number of filters enhances the network's capacity to learn complex relationships, it also introduces computational overhead. The choice of six filters is thus made to strike a balance between model complexity and computational efficiency: crucial considerations in battery state prediction tasks. The output of the CNN assessed using (14) is then fed to an LSTM layer with 400 hidden nodes to capture the temporal features of battery dynamics. The CNN-LSTM is trained for 500 epochs with a batch size of 64 using (13). The root mean square error (RMSE) used to evaluate the performance of the proposed scheme in predicting terminal voltage is as in (16),

RMSE = 
$$\sqrt{\frac{1}{K} \sum_{k=1}^{K} (V_{t(exp)} - V_{t(FO-PINN)})^2}$$
. (16)

The ratio of training: validation: testing is set as 0.7:0.05:0.25 from a total sample size of 640000 points. After training for 70% data, we evaluate the model's performance in the validation set. We feed the 5% input data (32000 sample points) through the network, compute the loss in terms of RMSE, and then use this information to adjust the hyperparameters. As the validation loss decreases while the training loss decreases, it indicates that the model does not suffer from overfitting. The resultant terminal voltages obtained from (15) are plotted in Fig. 7. The parameters of the IOM with constant parameters are  $R_0 = 0.0112, R_1 =$  $0.0059, R_2 = 0.0349, C_1 = 0.3379, C_2 = 444.372.$ RMSEs of IOM with constant parameters, IOM with SOCdependent parameters and the FO-PINN in terms of percentage errors are computed as 0.601%, 0.493% and 0.223%, respectively in the testing region. As the FO-PINN clearly mimics the experimental terminal voltage of the battery better than that of the IOMs without PINN, it validates our second contribution that integration of the FOM with PINN can capture unmodeled battery dynamics. As the SOC dependent FO-PINN yields improved voltage predictions, it in turn will be useful for SOC estimation in LFP batteries, where understanding the SOC inter-relationship with battery parameters will help understand the flat region dynamics; our third claim of contribution.



# C. Comparisons with existing methods

A comparison of the proposed scheme to existing modelling techniques applied to LFP batteries is provided in Table 1. The RMSEs are listed as reported in these works [6, 20, 22-25]. Comparison to our work reveals that our proposed

SOC dependent FO-PINN outperforms the existing methods for modelling LFP batteries. Specifically, the proposed modelling scheme achieves an RMSE of less than 0.25% - an order of magnitude less than most methods.

TABLE I. COMPARISON OF THE PROPOSED SCHEME WITH EXISTING MODELLING TECHNIQUES FOR LFP BATTERIES

| Work       | year | method   | FO  | RMSE   |
|------------|------|--|-----|--------|
| [22]       | 2023 | Pseudo-open-circuit voltage modelling  | No  | 3%     |
| [23]       | 2023 | Voltage interval at low state of charge  | No  | 2.67%  |
| [24]       | 2023 | Partial least squares regression models  | No  | 1.92%  |
| [6]        | 2023 | PDE based PINN   | No  | 0.42%  |
| [25]       | 2021 | Deep neural network  | No  | 2.03%  |
| [20]       | 2019 | CNN-LSTM   | No  | 2%     |
| This paper | 2023 | State dependent, fractional-<br>order physics-informed neural<br>network (FO-PINN) | Yes | 0.223% |

#### V. CONCLUSION

A state-of-charge dependent, fractional-order physics-informed neural network is proposed to predict the terminal voltage of an LFP battery. The hybrid neural network is a CNN-LSTM architecture which is informed by the physical states of the FOM. Through experimental validations, it is proved that the new SOC dependent FOM can encompass battery physics better than integer-order models. Also, this improved FOM guided neural network yields an RMSE of 0.223% and thus outperforms several other existing modelling techniques of LFP battery. A future direction of work is to study a PINN architecture by incorporating a fractional-order circuit element in the mid frequency region to capture the battery dynamics and analyse its sensitivity.

### REFERENCES

- [1] LFP batteries are popular! Apple, Tesla and Volkswagen joined the game one after another, https://news.metal.com/newscontent/101505954/lfp-batteries-are-popular-apple-tesla-and-volkswagen-joined-the-game-one-after-another
- [2] Daimler to use LFP cells from 2024, https://www.electrive.com/2021/10/28/daimler-to-use-lfp-cells-from-2024/#:~:text=Mercedes%2DBenz%20will%20switch%20to,specifically%20announced%20for%20two%20models
- [3] The global race for battery production is underway, https://www.emergingtechbrew.com/stories/2022/01/28/the-globalrace-for-battery-production-is-underway?
- [4] H. Tu, S. Moura, Y. Wang, H. Fang, "Integrating physics-based modeling with machine learning for lithium-ion batteries," *Applied Energy*, vol. 329, pp. 120289, 2023.
- [5] G. E. Karniadakis, I. G. Kevrekidis, L. Lu, P. Perdikaris, S. Wang and L. Yang, "Physics- informed machine learning," *Nature reviews*, *Physics*, vol. 3, pp. 420-440, 2021.
- [6] P. Wen, Y. Zhi-Sheng, L. Yong, C. Shaowei, and Z. Shuai, "Fusing Models for Prognostics and Health Management of Lithium-Ion Batteries Based on Physics-Informed Neural Networks," arXiv preprint arXiv:2301.00776, 2023.
- [7] K. Boonma, M. Mesgarpour, J. M. NajmAbad, R. Alizadeh, O. Mahian, A. S. Dalkılıç,... & Wongwises, S. "Prediction of battery thermal behaviour in the presence of a constructal theory-based heat pipe (CBHP): a multiphysics model and pattern-based machine learning approach," *Journal of Energy Storage*, vol. 48, pp. 103963, 2022.

- [8] S. W. Kim, E. Kwak, J. H. Kim, K. Y. Oh, & , S. Lee, "Modeling and prediction of lithium-ion battery thermal runway via multiphysicsinformed neural network," *Journal of Energy Storage*, vol. 60, pp. 106654, 2023.
- [9] K. Fricke, R. Giorgiani do Nascimento, and F. Viana, "Quadcopter soft vertical landing control with hybrid physics-informed machine learning," *In AIAA Scitech 2021 Forum*, p. 1018, 2021.
- [10] R. Giorgiani do Nascimento, F. Viana, M. Corbetta, & C. S. Kulkarni, "Usage-based Lifing of Lithium-Ion Battery with Hybrid Physics-Informed Neural Networks," In AIAA AVIATION 2021 FORUM p. 3046, 2021.
- [11] W. Li, J. Zhang, F. Ringbeck, D. Jöst, L. Zhang, Z. Wei, & D. U. Sauer, "Physics-informed neural networks for electrode-level state estimation in lithium-ion batteries," *Journal of Power Sources*, vol. 506, pp. 230034 2021.
- [12] Y. Wang, G. Gao, X. Li, Z. Chen, "A fractional-order model-based state estimation approach for lithium-ion battery and ultra-capacitor hybrid power source system considering load trajectory," *Journal of Power Sources*, vol. 177, no. 2, pp. 314-322, 2020, https://doi.org/10.1016/j.jpowsour.2019.227543
- [13] L. Chen, W. Yu, G. Cheng, & J. Wang, "State-of-charge estimation of lithium-ion batteries based on fractional-order modeling and adaptive square-root cubature Kalman filter," *Energy*, vol. 271, pp. 127007, 2023
- [14] M. Borah, S. Moura, D. Kato, J. Lee, "A nonlinear fractional-order dynamical framework for state of charge estimation of LiFePO<sub>4</sub> batteries in electric vehicles", Modelling, Estimation and Control Conference, IFAC, Nevada, USA, 2023
- [15] Y. Wang, X. Han, D. Guo, L. Lu, Y. Chen, & M. Ouyang, "Physics-Informed Recurrent Neural Networks with Fractional-Order Constraints for the State Estimation of Lithium-Ion Batteries," *Batteries*, vol. 8, (10), pp. 148, 2022.
- [16] Y. Wang, X. Han, L. Lu, Y. Chen, & M. Ouyang, "Sensitivity of Fractional-Order Recurrent Neural Network with Encoded Physics-Informed Battery Knowledge," *Fractal and Fractional*, vol. 6, (11), pp. 640, 2022.
- [17] C. A. Monje, Y. Chen, B. M. Vinagre, D. Xue, V. Feliu, Fractional-order Systems and Controls, *Springer-Verlag London Limited*. pp. 36-45, 2010.
- [18] K. Diethelm, N.J. Ford, A.D. Freed, "A predictor-corrector approach for the numerical solution of fractional differential equations,". Nonlinear Dynamics, vol. 29, pp. 3-22, 2002.
- [19] J. Chen, Y. Zhang, J. Wu, W. Cheng, and Q. Zhu, "SOC estimation for lithium-ion battery using the LSTM-RNN with extended input and constrained output," *Energy*, vol. 262, p.125375, 2023.
- [20] X. Song, F. Yang, D. Wang and K. -L. Tsui, "Combined CNN-LSTM Network for State-of-Charge Estimation of Lithium-Ion Batteries," in *IEEE Access*, vol. 7, pp. 88894-88902, 2019, doi: 10.1109/ACCESS.2019.2926517
- [21] M. Aykol, C.B. Gopal, A. Anapolsky, P.K. Herring, B. van Vlijmen, M.D. Berliner, M.Z. Bazant, R.D. Braatz, W.C. Chueh, and B.D. Storey, "Perspective—combining physics and machine learning to predict battery lifetime," *Journal of The Electrochemical Society*, vol.168, no. 3, pp. 030525, 2021.
- [22] K. Zhang, R. Xiong, Q. Li, C. Chen, J. Tian, and W. Shen, "A novel pseudo-open-circuit voltage modeling method for accurate state-ofcharge estimation of LiFePO4 batteries," *Applied Energy*, vol. 347, pp. 121406, 2023.
- [23] Y. Ni, J. Xu, C. Zhu, H. Zhang, Y. Yu, K. Song, and C. Wu, "Rapid estimation of residual capacity for retired LiFePO4 batteries using voltage interval at low state of charge," *Energy Storage Materials*, vol. 55, pp. 463-478, 2023.
- [24] L. Beslow, S. Landore, and J.W. Park, "Statistical Modeling Procedures for Rapid Battery Pack Characterization." *Batteries*, vol. 9, pp. 437, 2023.
- [25] J. Tian, R. Xiong, W. Shen, and J. Lu, "State-of-charge estimation of LiFePO4 batteries in electric vehicles: A deep-learning enabled approach." *Applied Energy*, vol. 291, pp. 116812, 2021